

## Shaping and Patterning Gold Nanoparticles *via* Micelle Templated Photochemistry

F. Kundrat,<sup>a</sup> G. Baffou<sup>b</sup> and J. Polleux<sup>\*a,c</sup>

<sup>a</sup> Max Planck Institute of Biochemistry, Department of Molecular Medicine, 82152 Martinsried, Germany.

<sup>b</sup> Fresnel Institute UMR 7249, CNRS, Aix-Marseille Université, Ecole Centrale Marseille, 13013 Marseille, France.

<sup>c</sup> Center for NanoScience, Ludwig Maximilian University, 80799 Munich, Germany.

†Electronic Supplementary Information (ESI) available: Additional SEM, TEM and extinction measurements further describe the mechanism of the reported photochemical approach. See DOI: 10.1039/x0xx00000x

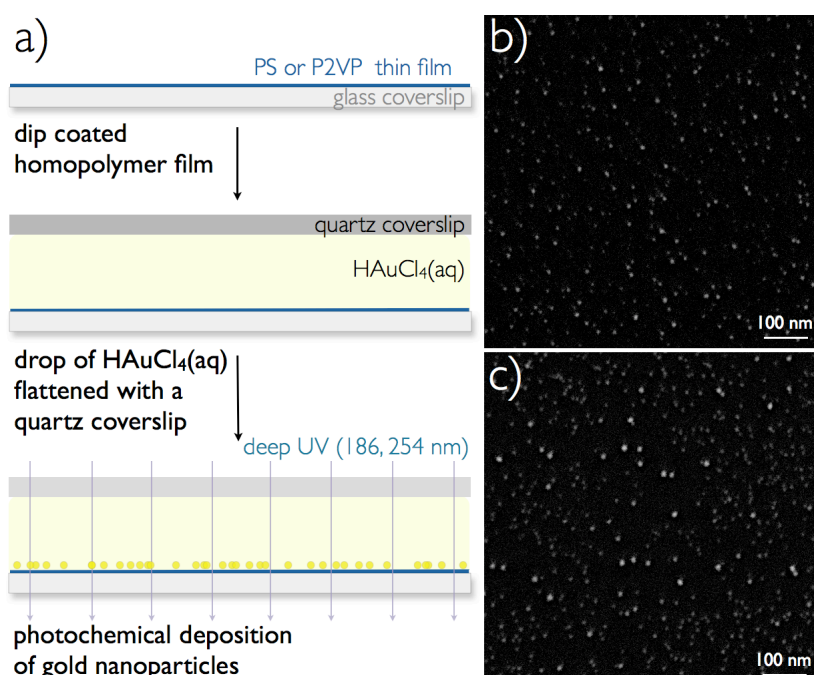


**Figure S1.** Photochemical deposition of gold nanoparticle monolayers on homopolymer thin films. a) Schematics describing the experimental procedure necessary to fabricate plasmonic substrates. SEM images displaying gold nanoparticles supported on b) PS- and c) P2VP-coated glass after 4-min deep UV irradiation.

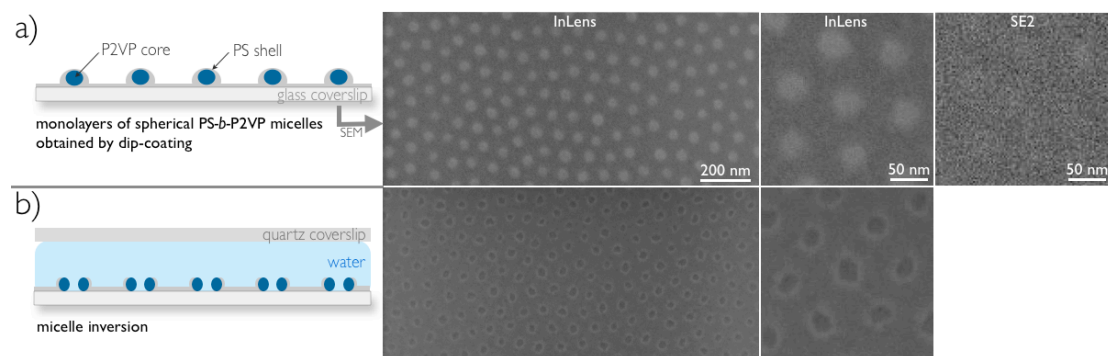


**Figure S2.** Water-mediated micelle opening. Schematics and SEM images illustrating the evolution of unloaded PS-*b*-P2VP micelles a) before and b) after morphology reconstruction induced by their immersion in water for 4 min. These images display a quasi-hexagonally ordered micellar monolayer, which becomes porous due to water-mediated swelling of the P2VP block, thereby rupturing the PS shell to finally form ring-like structures.

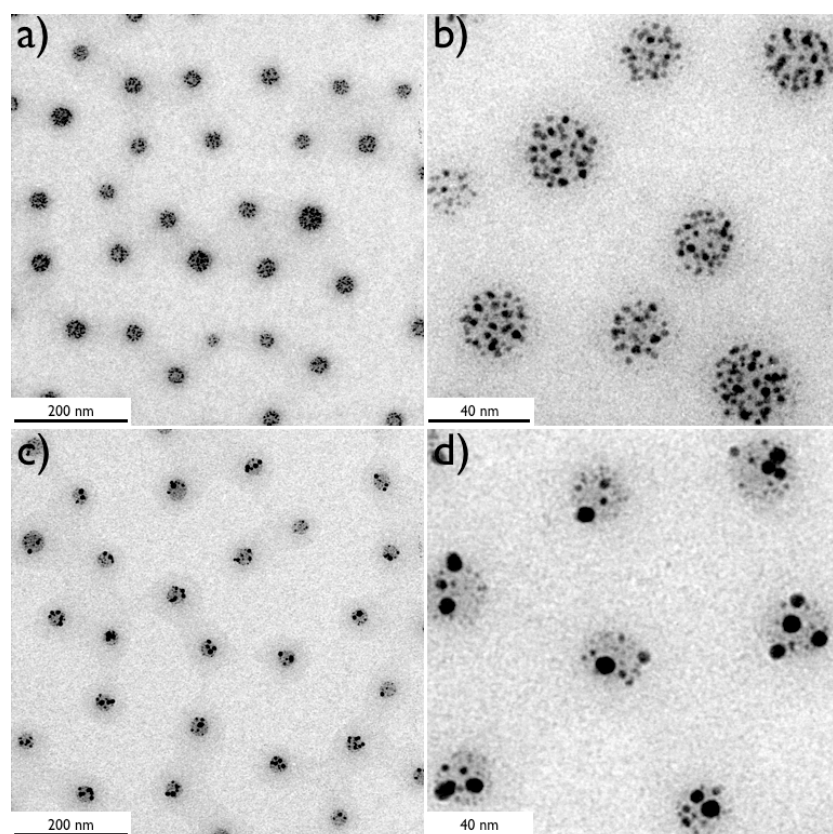


**Figure S3.** Photochemical growth of gold nanoparticles within micelles. Transmission electron microscopy (TEM) of gold-loaded micelles deposited on a copper grid coated with a SiO<sub>2</sub> film a),b) before and c),d) after deep UV illumination for 4 min in water.

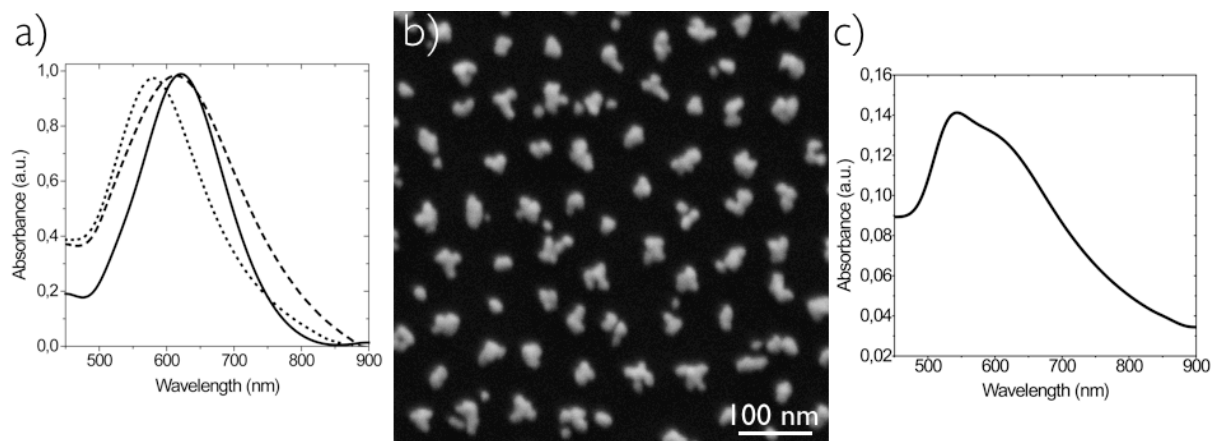


**Figure S4.** a) Normalized extinction spectra of gold potatooids grown for 10 (dots), 40 (dashes) and 90 min (line) in a mixture of gold aqueous solution and ethanolamine. b) SEM images displaying gold nanostructures prepared upon inverting the two last processing steps in comparison to the protocol described in Figure 1. c) Extinction spectrum of the gold nanostructures displayed in b).

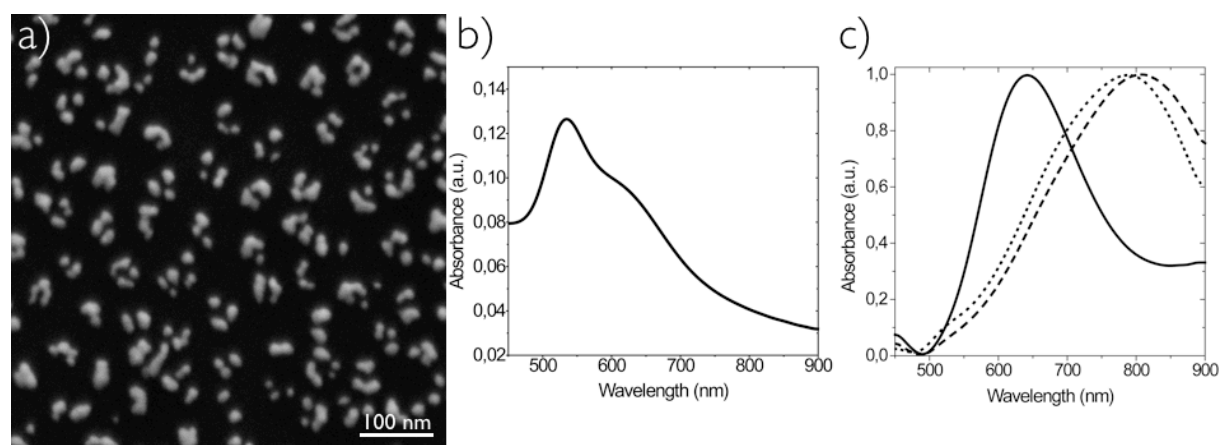


**Figure S5.** a) SEM images displaying gold nanostructures prepared upon inverting the two last processing steps in comparison to the protocol described in Figure 4. b) Extinction spectrum of the gold nanostructures displayed in a). c) Normalized extinction spectra of gold nanorings grown for 10 (dots), 30 (dashes) and 90 min (line) in a mixture of gold aqueous solution and ethanolamine.

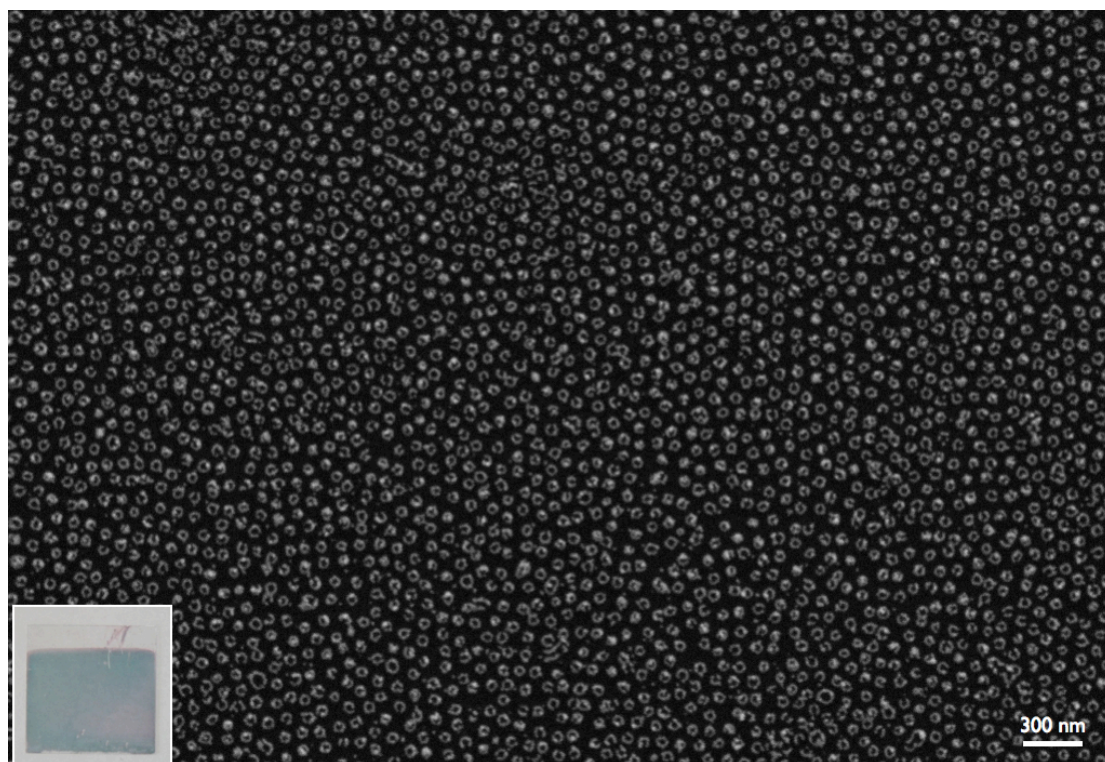


**Figure S6.** SEM image showing an overview of a uniform gold nanoring array. Inset displays an 18x18 mm glass coverslip coated with the nanoring array.

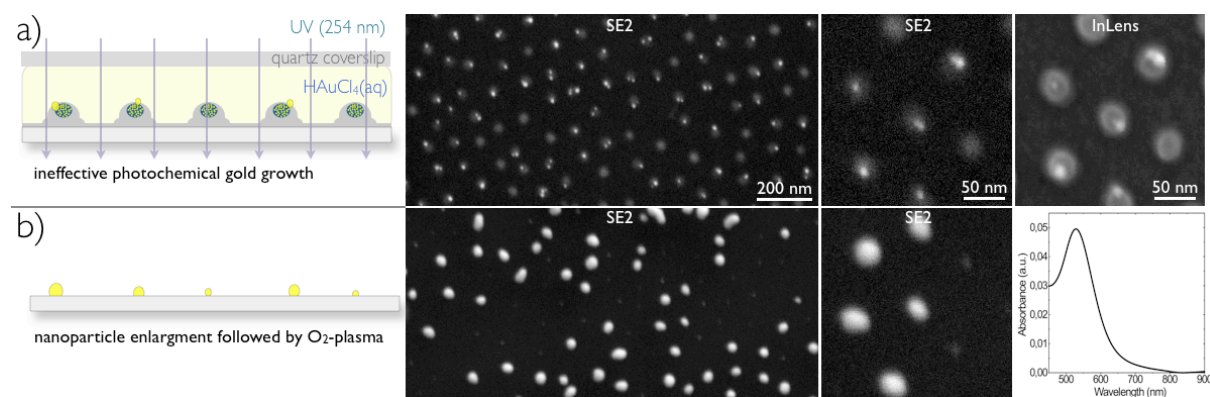


**Figure S7.** Monochromatic illumination ( $\lambda = 254$  nm) does not enable the fabrication of gold nanoring arrays. Schematics and SEM images illustrating the evolution of the nanostructured substrate upon a) deep UV illumination and b) electroless deposition followed by  $O_2$  plasma etching. The extinction spectrum of the gold nanoarrays is shown in b).

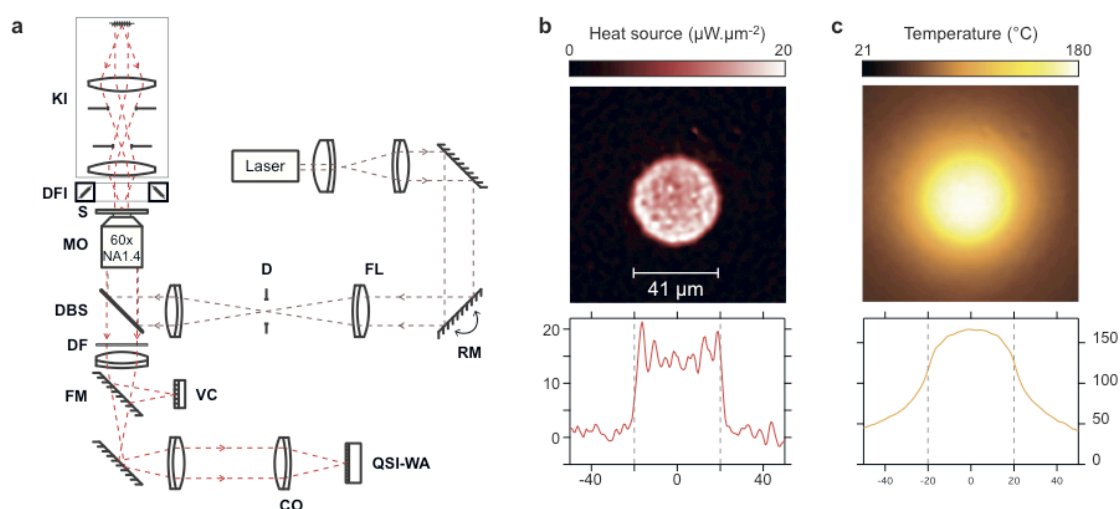


**Figure S8.** a) Schematic of the optical setup used for thermal microscopy measurements. KI: Köhler illumination, DFI: Dark Field Imaging. S: Sample, DBS: Dichroic Beam Splitter, DF: Dichroic Filter, FM: flip mirror, VC: Video Camera, CO: Camera Objective, QSI-WA: Wavefront analyzer based on Quadriwave Shearing Interferometry. D: Diaphragm, FL: Flip Lens, RM: Rotating Mirror. b) Map of the heat source density. c) Map of the temperature distribution. Figures b) and c) correspond to the same measurement of a laser beam (41  $\mu\text{m}$  in diameter,  $\lambda = 736$  nm, 63 mW) impinging on a potatoid substrate.